Third International Conference on CFD in the Minerals and Process Industries
CSIRO, Melbourne, Australia
10-12 December 2003

DEVELOPMENT OF A MATHEMATICAL MODEL OF FLASH SMELTING AND CONVERTING PROCESSES

Jussi VAARNO[1], Juha JÄRVI[1], Tapio AHOKAINEN[2], Toni LAURILA[3] and Pekka TASKINEN[1]

[1] Outokumpu Research Oy, P.O. Box 60, FIN-28101 Pori, FINLAND
[2] Outokumpu Technology Oy, P.O. Box 862, FIN-02201 Espoo, FINLAND
[3] Tampere University of Technology, Institute of Physics, Optics Laboratory, P.O. Box 692, FIN-33101 Tampere, FINLAND

ABSTRACT

Outokumpu has been developing mathematical models for concentrate and matte combustion continuously during the past decade. From the perspective of end users, process developers and designers, the major recent development step was the implementation of a model written for commercial CFD software CFX4 for FLUENT 6.1. This development allows one to benefit from flexible unstructured meshing and numerous general physical features implemented in FLUENT software.

In the field of model validation recent work has concentrated on particle temperature measurements. A measurement technique was applied in a small laminar flow reactor, which simulates the reaction shaft conditions for particles in a commercial-scale flash smelter. Two-color particle pyrometry allows simultaneous measurement of the temperature and size of individual reacting particles. The measured values were compared with the simulated ones.

Further development of model features has concerned radiation and particle-tracking models. New models were applied for a more accurate description of the radiative properties of a suspension. Particle–particle and particle–wall interactions were found to have a significant effect in physical experiments on flow dynamics near the burner. These effects are ignored in the standard particle-tracking model and therefore additional models are needed.

NOMENCLATURE

D diameter of the particle,
$e_{b\lambda}$ black body emission
$f(D)$ particle size distribution function
K_a absorption coefficient for gas phase
L path length of the radiation
m particle refraction index ($m = n - ik$)
N number of particles in unit volume
Q_β spectral absorption, scattering or extinction efficiency
T temperature
α absorptivity of the gas
$\kappa_{a\lambda}$ spectral absorption coefficient
$\kappa_{s\lambda}$ spectral scattering coefficient
$\kappa_{e\lambda}$ spectral extinction coefficient
λ wavelength of radiation

INTRODUCTION

The Outokumpu flash smelting process was developed at Harjavalta in 1949. Today it is has become the most widely used copper making process worldwide (about 50 % of global primary copper production and 30% of nickel, in more than 40 smelters) and is the state-of-the-art process as well as being the BAT in copper and nickel smelting (Kytö et al., 1997).

A typical flash smelting furnace is shown schematically in Figure 1. The refractory-lined furnace vessel is composed of three sections: reaction shaft, settler and uptake shaft. In the flash smelting process, a sulfidic feed mixture is distributed through the top of the reaction shaft by a concentrate burner, where the correct design is vital to furnace operation (Varnas, et.al, 1998). The concentrate burner consists of several concentric ducts through which the process gas and the concentrate are blown and mixed in the furnace. The main task of the burner is to produce an optimal suspension of solid particles and oxygen-enriched process air in the reaction shaft. Individual particles heat up as they fly about in the furnace and after ignition they start to combust with oxygen in the process gas (Jokilaakso et al, 1991). The combustion reactions with fine (< 100 μm) sulfides are very rapid and a substantial amount of heat is released, which leads to the complete melting of the combusting particle, as well as that of the other materials introduced in the feed mixture. The molten particles flow downstream and they are collected in the settler, where silicate slag and sulfidic matte layers are separated. The off-gas (mainly an SO_2 – N_2 mixture) flows through the uptake to the waste heat boiler, where it is cooled down and its heat content is recovered as steam (Yang et al., 1999).

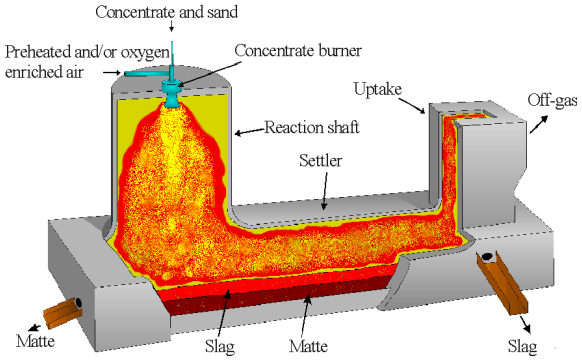

Figure 1: Flash smelting furnace with its main sections and material flows

Since its first industrial application, the process and its core equipment have been developed continuously to achieve low energy consumption, low environmental

emissions and a high level of occupational safety (Hanniala et al., 1999).
To assist this development, chemical and physical models have been developed aiming to depict various processes occurring inside the smelter. For the reaction shaft there are dedicated models for chemical reactions (Peuraniemi and Jokilaakso, 2000, Peuraniemi et al., 1999) and radiative heat transfer (Ahokainen, 2002).
These models are applied to numerical simulations. For this purpose, a mathematical model for copper flash smelting and flash converting was developed at the Helsinki University of Technology during the past decade (Järvi et al., 1998, Ahokainen and Jokilaakso, 1998).
The model can be used for simulating fluid flow, heat transfer and particle combustion in flash smelting and the flash converting furnace. The modeling work is done with commercial computational fluid dynamics software, which solves the flow equations for the process gas and the equations of motion for the particles. A particle combustion model (Flash smelting model) has been developed based on experimental work (Peuraniemi and Jokilaakso, 2000, Peuraniemi et al., 1999) and is connected to FLUENT using user-defined functions for particle law and source terms for the mass, momentum and enthalpy of the gas phase.
The aim of this article is to review the latest development work done for the FLASH model, i.e. mathematical models used in the Outokumpu flash furnace simulation.

MODEL DESCRIPTION

General model

The FLASH code calculates the changes in temperature and the composition of chalcopyrite ($CuFeS_2$), chalcocite (Cu_2S), copper matte ($Cu_2S{\cdot}yFeS$) and inert (SiO_2) particles as they move in the gas stream. The particle temperature is obtained from the particle heat balance which represents the heat transfer between the particle and its surroundings by radiation, convection and generated (or consumed) heat caused by chemical reactions. Heterogeneous reactions between the gas phase and the particle are described with the shrinking core model (Järvi et al., 1998, Ahokainen and Jokilaakso, 1998). The chemical reactions are controlled by a combination of oxygen mass transfer from bulk gas to the particle surface, oxygen transfer through the product layer to the reaction surface, and the chemical reaction rate. Based on the mass transfer calculation, oxygen consumption and sulfur dioxide formation is calculated.
In simulation, a solid feed mixture can contain different types of particles: chalcopyrite, chalcocite or inert. Sulfide particles can also have some amount of iron sulfide and silica inside the particle. Each type of particle can have a different chemical composition and its own particle size distribution.
The FLASH model was originally written for PHOENICS software and later it was translated into CFX4. In 2002, the code was implemented for FLUENT 6.1 software. The latest implementation was done entirely with user-defined functions while the earlier versions were partly written into the source code of the general CFD software.
The major reason for transferring the code to FLUENT 6.1 was the flexibility of unstructured meshing and hybrid meshing. The flash smelting reactor has great geometrical scale differences. The concentrate burner has complex geometry with relatively small details while the meshing of the rest of the reactor is much less demanding. Therefore, with a combination of unstructured mesh in the burner region and structured mesh in the shaft and settler, a good quality mesh with a reasonable total number of nodes may be produced for a Flash smelting or Flash converting application in less than twenty man-hours. An example of a computational grid in the concentrate burner area is presented in Figure 2.
The other reason for rewriting the code was the growing demand to include additional hydrocarbon fuel combustion in simulations. The latest implementation of the FLASH model (unlike earlier versions) includes activation of the carbon, oil and homogenous combustion models incorporated in the general solver.

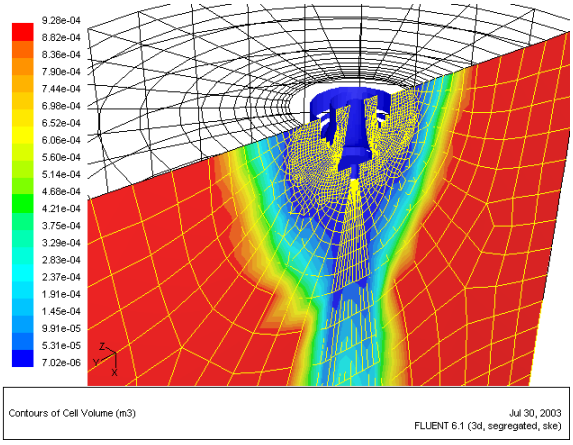

Figure 2: An example of a computational hybrid grid around the FS furnace concentrate burner.

Particle-particle-wall interactions

The mixing of process gas and concentrate or matte particles in the Flash smelting or Flash converting furnace is assisted by a distribution cone in the concentrate burner. Particles falling from the vertical feed tube collide into the distribution cone, which turns most of the vertical momentum of the free fall into a horizontal direction and ejects particles into the downward-oriented process gas jet.
In laboratory experiments particles have been shown to form a high particle concentration layer on top of the distribution cone surface. A high solids concentration layer extends from the rim of the distribution cone further towards the furnace. This particle veil, as it is termed, is dense enough to stop particles from falling near the feed tube that passes the distribution cone. The suspension layer is also thick enough effectively to level out the differences in the momentum of different-sized particles being ejected from the distribution cone.
The effects of these phenomena are shown in Figure 3 (left), in which a particle stream in a laboratory- scale FSF model is photographed in a laser sheet.
The FLASH model is based on a particle-tracking procedure that does not take into account any particle-particle interaction. Furthermore, the default particle–wall interaction is too simplified to describe the collisions of the particles with the distribution cone properly. These collisions play a critical role in transferring the particle potential energy into horizontal penetration energy.
Due to this oversimplified approach, the formation of a high particle concentration layer and veil cannot be modeled with a standard particle-tracking model. This is evident when comparing a simulated volume fraction of

particles with a photographed particle stream, as presented in Figure 3.

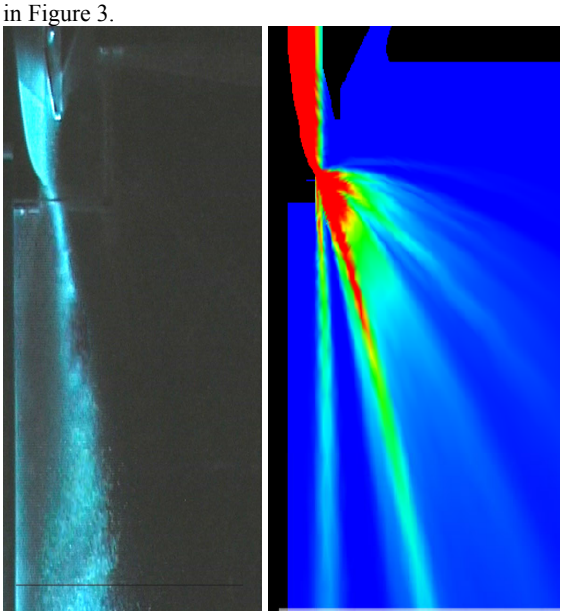

Figure 3: Photographed and simulated particle stream in a laboratory-scale FSF model.

To overcome this inaccuracy new features are to be added, according to the presentation of Triesch and Bohnet (1999), to the standard particle-tracking model of Fluent Inc. (2003).

In the approach of Triesch and Bohnet, the wall surface structure (Sommerfeld and Zikovic, 1992, Frank and Petrak, 1990) and particle angular velocity are taken into account in the calculation of post-collision velocities by the laws of impact established by Tsuji et al. (1985). These laws differentiate between sliding collision and adhesive impact collision.

Particle-particle collisions are taken into account by calculating the collision probability in each time step of the tracked particle and the numerically created "colliding particle". Post-collision velocities and contact velocities are calculated according to the impact laws presented by Triesch and Bohnet (1999).

Triesch and Bohnet (1999) have successfully implemented these models in version 4.4 of FLUENT but the implementation is not available for FLUENT 6.1, which is used by the FLASH model. Transferring these models to FLUENT 6.1 has now been done and the re-implementation is now in the testing phase.

Model for gas radiation properties

For modeling gas radiation properties, calculation of the absorptivity (α) of an arbitrary gas mixture was taken as the starting point. When the path length (L) of the radiation is known, the absorption coefficient (K_a) can be calculated from the absorptivity using the equation $K_a = -\ln(1 - \alpha)/L$. A sub-model for K_a was constructed. Input data for the model are the gas composition, pressure, temperature, radiation path length (cell size), and the corresponding reference values of these variables. The model was constructed for an arbitrary gas mixture, and the data was provided for six gas components, namely H_2O, CO_2, CO, NO, SO_2, and CH_4.

Calculation of the absorptivity is carried out using a block-approximation model, where the infrared part of the wave number spectrum (1–8500 cm^{-1}, 1–10^4 μm) is divided into blocks specific for each gas component at a particular temperature and pressure. Absorptivity of the gas mixture is then deduced by calculating the relative proportion of the blocks of each component from the black body emission at a specified temperature and pressure. Single gas component absorption and the block limits are calculated with the Exponential Wide Band Model (EWBM). In this calculation, the EWB model of Edwards and Balakrishnan (1973) and the approximation of Lallemant and Weber (1996) for band intensity are combined.

The total emissivity of the gas components and gas mixtures were calculated with the model at different temperatures and pressures and the results were compared with data found in the literature. The gases studied were CO_2, H_2O, SO_2, CH_4 and CO, and a mixture of CO_2 and H_2O. Differences in the emissivity values between the model predictions and tabulated data were found especially for the gas components that have not been extensively studied (CO, CH_4 and SO_2). Most of the emissivity values published in the literature have been extrapolated from experimentally determined low temperature values to higher temperatures. Thus, they may contain large errors and cannot be used to judge the model predictions at high temperatures. For these gases, single-band absorption values predicted by the model were compared to experimentally measured absorptivities and good agreement was found at low temperatures. It was concluded that the differences between the predicted and published emissivities were mainly due to poor temperature corrections used in the published data. The model-predicted emissivities of the well-known gases (CO_2, H_2O) and CO_2-H_2O mixture were found to match well or excellently with the data published in the literature. In Figure 4, a comparison of the model-predicted emissivity (EWBM) of a CO_2-H_2O mixture with the literature data is shown for different pL conditions.

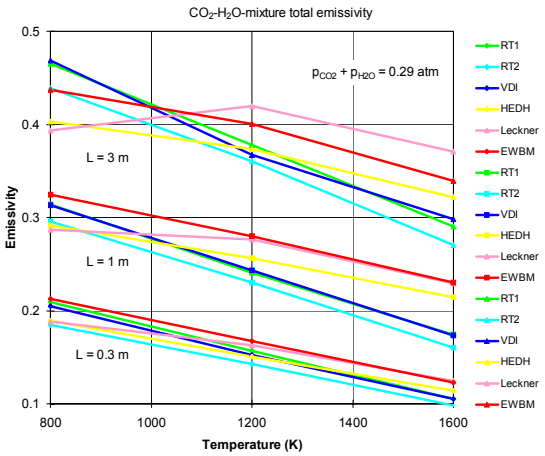

Figure 4: CO_2-H_2O mixture emissivity chart. EWBM = Model predictions. Other legends refer to literature: RT1, RT2 = Hottel and Sarofim (1967), VDI = VDI Heat Atlas (1993), HEDH = Heat Exchanger Design Handbook. (1983), Leckner = Leckner (1972).

Model for particle radiation properties

The sub-model for calculation of particle absorption and scattering coefficients is based on the equation

$$\beta_\lambda(m,N)=\int_0^\infty Q_\beta(D,\lambda,m)\frac{\pi D^2}{4}f(D)NdD \qquad (1)$$

where β_λ is spectral absorption coefficient $\kappa_{a\lambda}$, scattering coefficient $\kappa_{s\lambda}$ or extinction coefficient $\kappa_{e\lambda}$, Q_β is respective spectral efficiency, D is the diameter of the particle, $f(D)$ is the particle size distribution function, and N is the number of particles in the unit volume, m is the particle refraction index ($m = n - ik$) and λ is the wave length. Spectral efficiency may be calculated from the Mie theory (van de Hulst, 1981) for a single spherical particle. When the absorption and scattering efficiencies (Q) are known, equation (1) may be solved. However, the integration of the equation must be made over the particle size distribution $f(D)$ and the analytical solution exists only for constant size particles. By expressing $f(D)$ with an exponential function and performing a suitable change of variables it is possible to solve equation (1) numerically with simultaneous calculation of Q from the Mie equations. The resulting equation for κ's is valid for all wavelengths, but today the radiation simulation is seldom performed on spectral level. For current needs, the result is integrated over the wavelength resulting in the Planck absorption coefficient defined as:

$$\kappa_a^* = \frac{\int_0^\infty \kappa_{a\lambda}^* e_{b\lambda}(T)d\lambda}{\int_0^\infty e_{b\lambda}(T)d\lambda} \qquad (2)$$

where $e_{b\lambda}$ is the black body emission at a particular temperature T. Integration of equation (2) is done numerically inside the sub-model. The only problem is how to define the integration limits efficiently because the equation is solved many times at many different temperatures. In the sub-model, the integration limits for solving equation (2) are made scalable, and the integration is adjusted to cover 99% of the black body emission at each temperature. Then, the wavelength spectrum can be divided into less than 10, which reduces the numerical effort considerably.

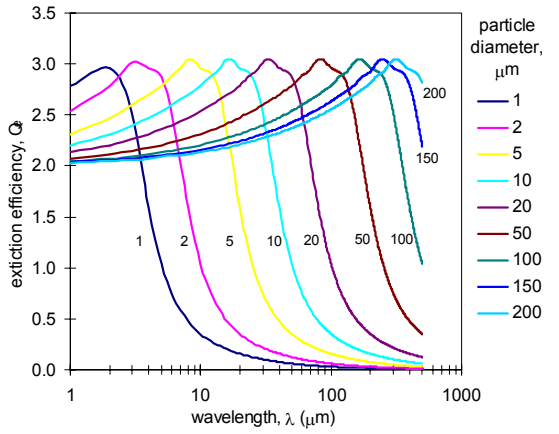

Figure 5: The effect of particle diameter on extinction efficiency (Q_e). Refraction index m = 2.02-0.8i.

In Figure 5, the extinction efficiency (Q_e), calculated with the model, is shown for different sizes of particle. It is obvious from this result that small particles attenuate radiation in low wavelength regions, whereas they become transparent to radiation as the wavelength increases. Figure 5 also shows that as the wavelength decreases, the extinction coefficient approaches the value of 2, which is the geometrical limit for "large particles" (when the size parameter $x = \pi D/\lambda$ is large).

EXPERIMENTAL

Throughout the development phase of the FLASH code the lack of temperature data has complicated the validation of the developed models. Therefore, while the latest model implementation was being verified, a new two-colour pyrometer was developed and applied for the measurement of individual chalcopyrite ($CuFeS_2$) particle temperatures and sizes in laboratory-scale tests.

Two-colour optical pyrometry measurements

Optical pyrometry is based on the detection of radiation from an object. For blackbody radiation Planck's well-known radiation law describes the energy distribution as a function of the object temperature and detection wavelength. However, real objects do not exhibit ideal blackbody radiation characteristics as the emissivity is always smaller than unity and may depend on wavelength, temperature, direction and surface conditions. Optical pyrometers operating at two or more distinct wavelengths provide at least partial compensation for these effects. In addition to temperature, the developed two-colour particle pyrometry also enabled the simultaneous in situ size measurements of reacting chalcopyrite particles. The intensity of the radiation emitted by a particle is proportional to the projected area of the particle. This allows particle size determination if the particle temperature and emissivity are known. The sizing method based on this interrelation is called pyrometric particle sizing (Joutsenoja et al., 1997, Joutsenoja, 1998).

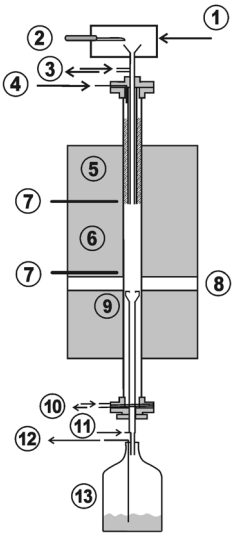

Figure 6: The laminar flow reactor: 1 carrier gas flow, 2 vibratory feeder, 3 feeding tube cooling water, 4 reaction gas inlet, 5 reaction gas heating, 6 reaction tube, 7 thermocouple, 8 optical access for pyrometric measurements, 9 sample collector, 10 cooling water, 11 quenching water inlet, 12 exhaust gas outlet, 13 sample container.

The copper sulfide particle temperature and size measurements were done in a laboratory-scale laminar flow reactor at the Laboratory of Materials Processing and Powder Metallurgy of the Helsinki University of Technology. The reactor is shown schematically in Figure 6.

The reactor consists of a feeder, a pre-heater, reaction gas inlets, a reactor tube, an electric heater, and a sample collector. The reactor has two temperature-controlled electrically heated zones. A vibratory feeder was used to feed the fuel particles into the water-cooled feeding tube with a small carrier gas flow of the same composition as the reaction gas. The distance between the exit end of the feeding tube and the optical detection ports was adjusted by moving the feeding tube.

The sample collector is located immediately downstream from the optical detection point. The reaction gas enters a sprayed water membrane at the entrance end of the sample collector. The reaction gas is cooled rapidly and all the chemical reactions are quenched. The water- containing particles are collected in a sample container and gases are exhausted through a filter and alkali bed.

Test Program

The conditions of the test program are shown in Table 1. The variable parameter was the oxygen concentration. The particles were prepared by milling the chalcopyrite ore and then enriching the copper concentration using a flotation process. The copper concentrate was dried, milled and sieved into the nominal size fraction of 53-74 μm. Particle size fractions were checked with a particle size analyzer. Solid reaction products were also collected during each test. The particle size distribution of the solid reaction product was also determined with the particle size analyzer.

Constants	Value
Total reaction gas flow	16 l/min (STP)
Average concentrate feed rate	0.4 g/min
Gas temperature	1273 K
Reaction distance	8 cm
Nominal particle size fraction	53-74 μm
Variables	Values
Initial oxygen concentration	10, 20, 50, 75 vol-%

Table 1: Experimental test conditions

Experimental results

The temperature and size distributions of reacting particles and SEM images of the solid reaction products were obtained from measurements taken under each process condition. The results are summarized in Table 2. One test lasted approximately 10 minutes and the mass of chalcopyrite particles processed within this time was 4.0 g. The number of particles detected by the pyrometer under each fixed process condition varied, but after the signal discrimination process several hundreds of particles were accepted typically for temperature and size determination.

Examples of the measured particle temperature and size distributions at varying oxygen concentrations are shown in Figure 7. The corresponding SEM pictures of the solid reaction products are also shown.

Process parameter		Particle color temperature	
O_2 (%)	T_g (K)	Med. T_p (K)	Max T_p (K)
75	1273	2287	2658
50	1273	2213	2558
20	1273	1693	2274
10	1273	1432	1717

Table 2: Summary of the results. The first two columns show the process variabless. The third column shows the median of the particle temperatures, and the fourth column the maximum temperature of the particles.

Comparison with Experimental Results

Sulfur removal comparisons between the numerical modeling and laboratory tests have show a good agreement in earlier studies (Järvi et al., 1998, Ahokainen and Jokilaakso, 1998). The temperatures of the individual particles were validated by simulating experimental conditions of the laminar flow furnace.

A comparison between the simulated and measured temperatures is shown in Figure 8. The detection limit of the pyrometer (illustrated with a black line in Figure 7) sharply cuts off particles smaller than 20 - 50 μm in the case of the 10 vol-% oxygen concentration. Therefore, the limitations of pyrometric particle thermometry and sizing must be kept clearly in mind when statistical parameters are calculated and used to compare the information of a particle temperature vs. size distribution, e.g. very different distributions can result with the same statistical parameters. In this case, the comparison of measured and the simulated temperatures are limited to maximum temperatures to ensure statistical equivalence.

Simulated and measured maximum temperatures have very good agreement, except in the case of the 20 vol-% oxygen concentration.

The simulated temperature history of a particle as a function of reaction distance is a good way to compare temperature values and SEM pictures. With a low oxygen concentration (10 vol-%) the particles are just starting to react more intensively and therefore temperatures are at a low level. When the particles reach the melting point, the reaction rate increases rapidly. In SEM micrograph Figure 7a only solid particles can be seen.

Based on the simulation, the smallest particles have already reacted and larger ones have not melted in the case of the 20 vol-% oxygen concentration. The biggest difference between the maximum and median temperatures and also between the measurements and simulation was obtained in this case. One possible explanation is the operation range near the particle melting point.

The highest temperatures for larger particles were attained with 50 vol-% oxygen, because they are then at the most aggressive reaction stage. The particles with originally a small diameter have already reacted completely and have lower temperatures. Small particles with high temperatures (shown e.g. in Figure 7c) are caused by a fragmentation of larger particles, which is not included in the simulation. Similar results were obtained with the highest 75 vol-% oxygen concentration.

Absence of fragmentation in the flash smelting model and possibly an irregularity in the vibratory feeding can cause some differences between simulated and experimental

results, but as a whole, very a good agreement was obtained.

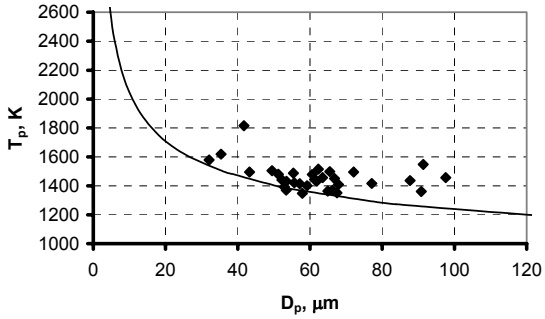

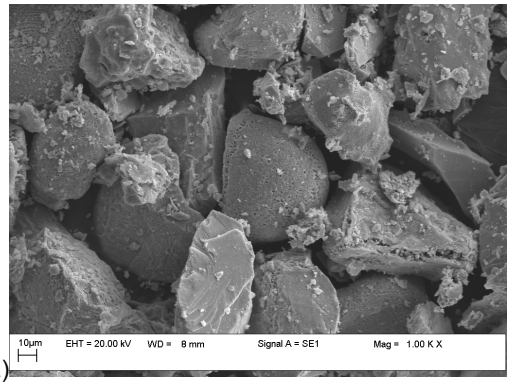

a)

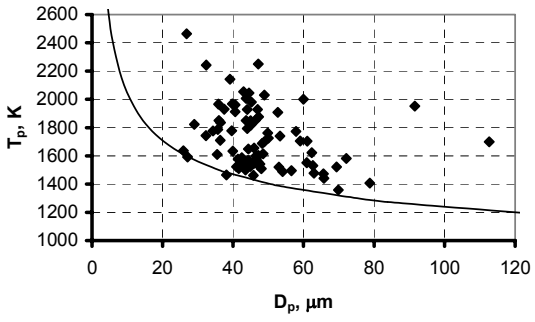

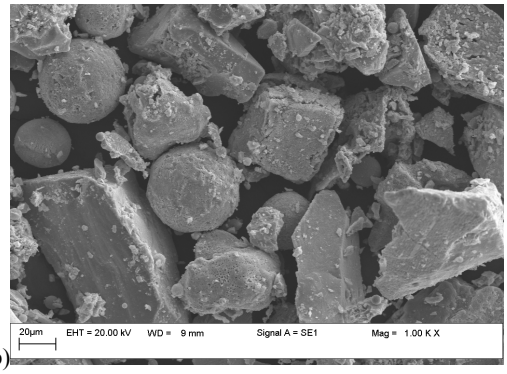

b)

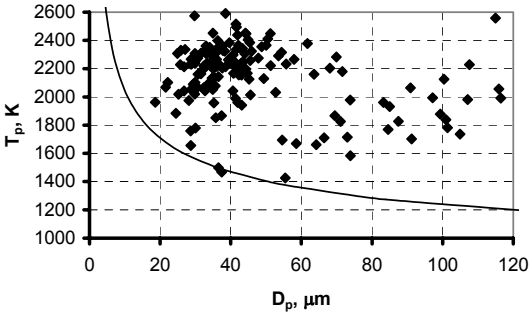

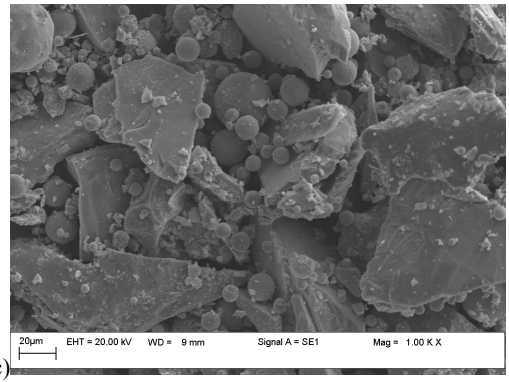

c)

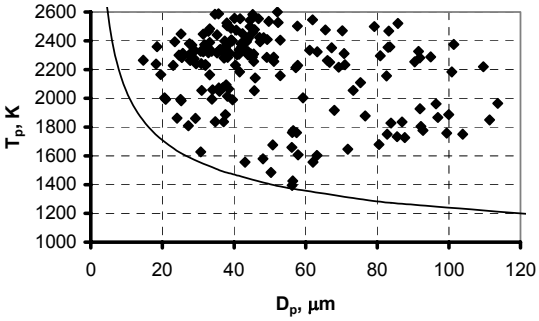

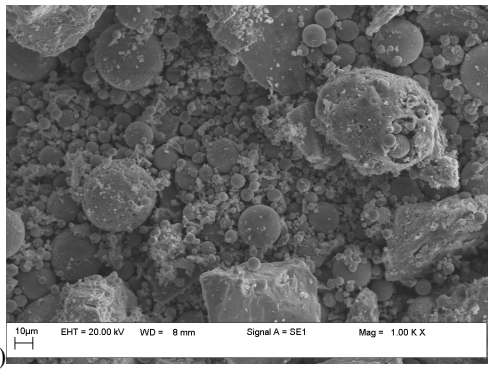

d)

Figure 7: Particle temperature and size distributions and corresponding SEM pictures of the solid reaction products at T_g=1273 K, 8 cm reaction distance, and an oxygen concentration of a) 10, b) 20, c) 50, and d) 75 vol-%.

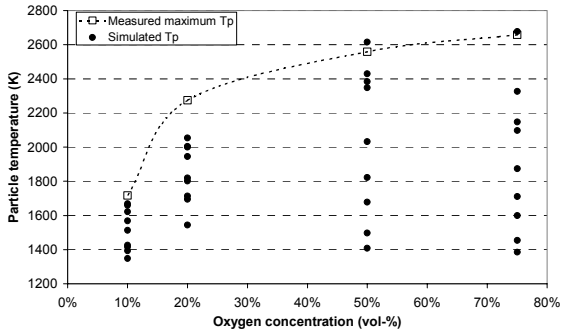

Figure 8: Measured maximum particle temperatures in laminar flow furnace at T_g=1273K, 8 cm reaction distance, oxygen concentrations of 10, 20, 50, and 75 vol-% and size fraction 53-74 μm and temperatures of 9 simulated particles representing fractions 40-80 μm passing corresponding distance (8 cm +/- 0.5 cm). Due to the individual history each simulated particle temperature varies in control point.

CONCLUSION

In this article the recent development of Flash smelting/converting model FLASH has been reviewed.

In order to validate the FLASH model, a two-color optical particle pyrometer was applied to measure the temperature and size of individual chalcopyrite particles in a laminar flow reactor. The measurements were made at a fixed gas temperature (1273 K), reaction distance (8 cm) and nominal particle size (53-74 μm). The variable parameter was the oxygen concentration (10, 20, 50 and 75 vol-%).

The measured particle temperatures ranged from 1400 K up to 2650 K, depending on the oxygen concentration. The measured particle sizes of the reacting particles ranged from around 10 μm up to 100 μm. The measured particle temperatures were compared with values predicted by the computational fluid dynamics model for flash smelting. The obtained agreement between the measurement results and the simulation was excellent.

The lead time demands set by the process design and development of Flash smelting technology required the re-implementation of the FLASH model in a commercial software package supporting unstructured and hybrid meshing.

The standard particle-tracking models of commercial CFD software packages do not allow the Flash smelting or Flash converting corcentrate burner modeling with an appropriate accuracy. Therefore, additional models for particle–particle and particle–wall interaction are needed in the future.

The increasing calculation power of modern computers and CFD packages enables the more accurate simulation of radiation properties of a chemically reacting suspension. For this purpose, models for estimating gas mixture emissivity and particle absorption and scattering coefficients have been developed.

ACKNOWLEDGEMENTS

This research was partly supported by the National Technology Agency of Finland (TEKES).

REFERENCES

AHOKAINEN, T. and JOKILAAKSO, A., (1998) "Numerical simulation of the Outokumpu flash smelting furnace reaction shaft", *Canadian Metallurgical Quarterly*, **37**, 275-283.

AHOKAINEN, T., (2002) "Radiation heat transfer in particle-gas suspension", *CODE: Technology programme for Modelling of Combustion Processes, Technical Review 1999-2002* (Ed. Partanen J.), TEKES, 377-388 (3).

EDWARDS, D.K. and BALAKRISHNAN, A., (1973), "Thermal radiation by combustion gases", *Int. J. Heat Mass Transfer*, **16**, 25-39.

Fluent Inc. (2003) "FLUENT documentation Release 6.1".

FRANK T.H. and PETRAK D., (1990), "Computersimulation der feststoffbeladenen Gasströmung im horizontalen Kanal mit Hilfe des Lagrange-Modells unter Berücksichtigung der Wandrauhigkeit", *Proc. IV 4. Int. Cong. Pneum. Transp*., Budapest, Hungary.

HANNIALA, P., HELLE, L. and KOJO, I., (1999) "Competitiveness of the Outokumpu Flash Smelting Technology Now and in the third Millennium", *Copper 99-Cobre 99 Int. Symp. – Vol V* (Ed. George, D., Chen, W., Mackey, P. and Weddick, A.), TMS, Warrendale (PA), 221-238

Heat Exchanger Design Handbook, (1983), Hemisphere Publishing Corporation, USA.

Hottel, H.C. and Sarofim, A.F., (1967), "Radiative Transfer", McGraw-Hill Book Company, USA.

JÄRVI, J., JOKILAAKSO, A. and AHOKAINEN, T., (1998)"Mathematical Modelling of Chalcocite Oxidation Reactions", *International Symposium on Computer Applications in Metallurgy and Materials Processing,* The Metallurgical Society of CIM, 19-29.

JOKILAAKSO, A., SUOMINEN, R., TASKINEN, P. and LILIUS, K., (1991), "Oxidation of chalcopyrite in simulated suspension smelting", *Trans. Inst. Min. Metall., Sect. C,* **100**, C79-90

JOUTSENOJA T. (1998), "Pyrometric thermometry and sizing of fuel particles in combustion", Ph.D. Thesis, Tampere University of Technology, Finland, 101.

JOUTSENOJA, T., STENBERG, J., HERNBERG, R. and AHO, M., (1997), "Pyrometric measurement of the temperature and size of individual combusting fuel particles", *Applied Optics*, **36**, 1525-1535.

KYTÖ, M., KOJO, I. and HANNIALA, P., (1997), "Outokumpu flash technology meeting the environmental and business challenges of the next century", *Metall,* **51**, 197-204

LALLEMANT and WEBER, (1996), "A Computationally efficient procedure for calculating gas radiative properties using the exponential wide band model", *Int. J. Heat Mass Transfer,* **39**, 3273-3286.

LECKNER, B., (1972), "Spectral Emissivity of Water Vapor and Carbon Dioxide". *Combustion and Flame,* **19**, 33-48.

MORGAN, G.J. and BRIMACOMBE, J.K., (1996) "Kinetics of the Flash Converting of MK (Chalcocite) Concentrate", *Metall. Trans. B*, **27B**, 163-175.

PEURANIEMI, E. and JOKILAAKSO, A., (2000), "Reaction Sequences in Sulphide Particle Oxidation", *EPD Congress 2000*, (Ed. Taylor, P.R.), TMS, Warrendale (PA), 173-187.

PEURANIEMI, E., JÄRVI, J. and JOKILAAKSO, A., (1999) "Behaviour of copper matte particles in suspension oxidation", *Copper 99-Cobre 99 Int. Symp. – Vol VI* (Ed. Diaz, C., Landolt, C. and Utigard, T.), TMS, Warrendale (PA), 463-476.

SOMMERFELD, M. and ZIKOVIC, G.,(1992), "Recent Advances in the Numerical Simulation Of Pneumatic Conveying Through Pipe Systems", *Computational Methods in Applied Sciences*, Elsevier Science Publishers, 201-212.

TRIESCH, O. and BOHNET, M., (1999), "CFD-Calculation of Pressure Drop for Pipe and Diffuser Gas-Solids Flow", *Proc. 2nd International Symposium on Two-Phase Flow Modelling and Experimentation*, (Ed. Celata, G.P. Di Marco, P. and Shah, R.K.), Edizioni ETS, Pisa, Italy 1343-1351.

TSUJI, Y. OSHIMA, T. and MORIKAWA, Y., (1985), "Numerical simulation of pneumatic conveying in a horizontal pipe", *KONA*, **3**, 38-51.

VAN DE HULST, H.C., (1981), "Light scattering by small particles", Dover Publications, Inc., New York.

VARNAS, S., KEMORI, N. and KOH, P., (1998), "Evaluation of Nickel Flash Smelting through Piloting and Simulation", *Metall. Trans. B*, **29B,** 1329-1343.

VDI Heat Atlas (1993), VDI-Verlag GmbH, Düsseldorf.

YANG Y., JOKILAAKSO, A., TASKINEN, P. and KYTÖ, M., (1999), "Using Computational Fluid Dynamics to Modify a Waste-Heat Boiler Design", *JOM*, **51**, 36-39.